Published in final edited form as:
Supramol Chem. 2015 January 1; 27(1-2): 65–71. doi:10.1080/10610278.2014.906601.

Enantiopure Cryptophane-^{129}Xe Nuclear Magnetic Resonance Biosensors Targeting Carbonic Anhydrase

Olena Taratula, **Yubin Bai**, **Edward L. D'Antonio**, and **Ivan J. Dmochowski***
Department of Chemistry, University of Pennsylvania, 231 South 34th St., Philadelphia, PA 19104

Abstract

The (+) and (−) enantiomers for a cryptophane-7-bond-linker-benzenesulfonamide biosensor (**C7B**) were synthesized and their chirality confirmed by electronic circular dichroism (ECD) spectroscopy. Biosensor binding to carbonic anhydrase II (CAII) was characterized for both enantiomers by hyperpolarized (hp) ^{129}Xe NMR spectroscopy. Our previous study of the racemic (+/−) **C7B** biosensor-CAII complex [Chambers, et al., J. Am. Chem. Soc. 2009, *131*, 563–569], identified two "bound" ^{129}Xe@**C7B** peaks by hp ^{129}Xe NMR (at 71 and 67 ppm, relative to "free" biosensor at 64 ppm), which led to the initial hypothesis that (+) and (−) enantiomers produce diastereomeric peaks when coordinated to Zn^{2+} at the chiral CAII active site. Unexpectedly, the single enantiomers complexed with CAII also identified two "bound" ^{129}Xe@**C7B** peaks: (+) 72, 68 ppm and (−) 68, 67 ppm. These results are consistent with X-ray crystallographic evidence for benzenesulfonamide inhibitors occupying a second site near the CAII surface. As illustrated by our studies of this model protein-ligand interaction, hp ^{129}Xe NMR spectroscopy can be useful for identifying supramolecular assemblies in solution.

Keywords

^{129}Xe NMR spectroscopy; xenon biosensing; hyperpolarization

Introduction

The need for molecular-based medical diagnostic and treatment options (i.e., "molecular medicine") motivates the development of spectroscopic and imaging techniques that can identify trace bio-analytes in complex media. In clinical practice, magnetic resonance imaging (MRI) is commonly used to scan deep tissues in human patients noninvasively and with high spatial resolution (< 100 μm^3 per voxel). The challenge of identifying abnormal tissue based on proton signals from surrounding water and fat molecules often requires the use of contrast agents, e.g., gadolinium chelates and iron-oxide-based agents (1, 2). This combination typically provides valuable structural-anatomical information that helps to differentiate diseased from healthy tissues, but offers few additional molecular details. In particular, there have been challenges in developing contrast agents for *in vivo* imaging of medically relevant biomarkers, such as proteins. The importance of *in situ* molecular data for early and accurate diagnosis of disease continues to drive the development of

*Corresponding author: Dmochowski, Ivan J.ivandmo@sas.upenn.edu.

complementary, molecule-specific, high-sensitivity contrast agents and detection strategies for MRI (3-7).

One option for increasing the magnetic spin reservoir is to use hyperpolarized (hp) nuclei (spin-1/2 options include ^{13}C, ^{3}He, ^{129}Xe), which achieves magnetic resonance signal enhancements of several orders of magnitude compared to thermally equilibrated spin populations. ^{129}Xe is an inert gas, and is abundant and readily harvested from the Earth's atmosphere. ^{129}Xe can be hyperpolarized to near unity by spin-exchange optical pumping (8). Based on its significant polarizability, ^{129}Xe binds void spaces in appropriately sized organic host molecules, e.g., cryptophane-A (9-14). Functionalizing the cryptophane produces significant chemical shift changes (15) (> 300 ppm window, important for simultaneous detection of multiple species in aqueous solution) and also imparts control over supramolecular interactions, which enables the sensitive hp ^{129}Xe NMR detection of proteins, DNA, membranes, or metal ions in solution (16-18).

Our laboratory (7, 13, 15, 19, 20) and others (6, 17, 18, 21-29) have explored biosensing and bioimaging applications with hyperpolarized ^{129}Xe magnetic resonance. A particular focus has been the development of hyperpolarized ^{129}Xe NMR biosensors for biomedically relevant protein targets, which has led to the attachment of protein-targeting moieties to high-xenon-affinity host molecules. Cryptophane-A is chiral, but most studies are performed with racemic cryptophane as synthetic methods for generating useful quantities of enantiopure cryptophane material have been lacking until recently (30, 31). One protein target is carbonic anhydrase (CA), which plays important physiologic roles in carbon dioxide transport and pH homeostasis (32). Moreover, several CA isozymes are upregulated in cancer and other diseases, making CA a useful biomarker. Small-molecule drugs targeting CA typically contain a benzenesulfonamide moiety, which can coordinate as the deprotonated sulfonamidate to a buried Zn^{2+}. This enzyme active site resides ~15 Å from the protein exterior surface. For these reasons, racemic cryptophane biosensors were generated in our lab with linkers of 6, 7, or 8 bonds (C6B, C7B, C8B) separating the cryptophane from the benzenesulfonamide terminus (33). This range of linker lengths was chosen for delicately tuning the interaction between cryptophane and the CA active-site channel. The three racemic biosensors were confirmed by isothermal titration calorimetry to bind with nanomolar dissociation constants to CA I and II. A 1.7-Å resolution structure determination of the 8-bond-linker biosensor, C8B, crystallized with CAII confirmed sulfonamidate-Zn^{2+} coordination, as well as occupancy of the biosensor within the active-site channel (34).

The racemic cryptophane biosensors yielded ^{129}Xe NMR chemical shifts that varied considerably depending on the length of the linker as well as the CA isozyme (CAI vs. CAII) (33). When complexed with CAII, racemic **C7B** showed a bound resonance at 67.0 ppm, and a second bound resonance at 71.2 ppm ($\Delta\delta$ = 7.5 ppm, relative to the unbound resonance at 63.7 ppm). This protein-mediated shift was the largest ever reported for a xenon biosensor. We hypothesized that the two bound resonances were the result of diastereomerism, with the (+) and (−) **C7B** enantiomers interacting differently with the chiral CAII active site. Here, to test that hypothesis, we synthesized the enantiopure **C7B**

biosensors and performed hp ^{129}Xe NMR spectroscopy for each enantiomer in the presence of CAII.

Results and discussion

Synthesis

The final steps in enantiopure **C7B** biosensor synthesis are outlined in Scheme 1. The enantiopure precursors, tripropargyl cryptophanes **1a** and **1b**, were prepared in 9 overall steps in good yield. Briefly, this followed our previously published synthetic routes for racemic trihydroxy cryptophane (6 steps), subsequent installation of three Mosher's acids, purification of cryptophane diastereomers by column chromatography, removal of Mosher's acids to reveal enantiopure cryptophane (deprotection step), and, finally, installation of three propargyl moieties to give **1a** (−) and **1b** (+) (31). The azido-functionalized, *para*-substituted benzenesulfonamide linker **2** was readily synthesized in 1 step from the amine analogue to provide a 7-bond spacer between the cryptophane and benzenesulfonamide recognition unit (33). Linker **2** was then reacted with **1a** and **1b** via a copper (I)-catalyzed [3 + 2] cycloaddition process, to give the functionalized enantiopure cryptophanes **3a** and **3b,** as previously described for racemic tripropargyl cryptophane (33). Finally, to increase water solubility, the enantiopure cryptophanes **3a** and **3b** were reacted with excess 3-azidopropionic acid **4** by the same copper (I)-catalyzed [3+ 2] cycloaddition process to give the pair of water-soluble enantiomers (−)-**C7B** and (+)-**C7B** in ~50% yield.

Circular dichroism spectroscopy

The enantiopurity of the isolated enantiomers (−)-**3a** and (+)-**3b** as well as enantiomers (−)-**C7B** and (+)-**C7B** was confirmed by electronic circular dichroism (ECD) spectroscopy showing the same peaks with opposite sign (Fig. 1). The ECD spectra, recorded in 1,4-dioxane (a solvent that is too large to enter the cryptophane cavity), were mirror images within experimental error, as expected for pairs of enantiomers. The molar ellipticity values, both in sign and magnitude, also agreed well with those measured for other chiral cryptophanes of C_1 symmetry (35). In the absence of a X-ray crystal structure for the isolated enantiomers, the structural assignment for the two enantiomers was made by reacting (+)-trihydroxy cryptophane with methyl iodide to yield (+)-cryptophane-A. Its recorded ECD spectrum was found to be opposite of the previously reported spectrum for (−)-cryptophane-A (36).

^{129}Xe NMR spectroscopy

HP ^{129}Xe NMR spectra were collected for both **C7B** enantiomers, either alone in solution or complexed with 0.5 or 1.0 equiv. of CAII (Fig. 2). As expected, one ^{129}Xe NMR peak was observed for xenon bound to each enantiomer tumbling freely in solution: (−) 64.0 ppm and (+) 64.8 ppm. These chemical shifts are identical within experimental error (± 0.5 ppm) based on the temperature variability (297 K ± 1 K) within the NMR spectrometer. These chemical shifts were also in agreement, within error, of the “free” peak at 63.9 ppm observed previously for racemic **C7B** (33). However, titration of 0.5 or 1.0 equivalents of CAII into the enantiopure biosensor solutions led to the unexpected finding of two “bound” peaks for both **C7B** enantiomers. This ran counter to expectations of the (−) enantiomer

producing one “bound” peak and the (+) enantiomer producing the other “bound” peak previously seen for ^{129}Xe@racemic-**C7B** (33). Instead, stoichiometric ^{129}Xe@(−)-**C7B**:CAII sample gave two similarly intense and broad peaks at 71.6 and 67.9 ppm and ^{129}Xe@(+)-**C7B**:CAII gave a narrow-linewidth peak at 67.8 ppm and smaller peak at 66.6 ppm. The hp ^{129}Xe NMR spectrum of the stoichiometric ^{129}Xe@racemic-**C7B** complex was measured in the same buffer conditions as the enantiopure biosensors, and gave peaks at 72.5 and 67.9 ppm (Fig. 3), in agreement with our previous report (33). Thus, the observation of two “bound” peaks at ~72 ppm and ~68 ppm is consistent across the enantiopure ^{129}Xe@(−)-**C7B**:CAII and racemic samples. Substantial amounts of “free” biosensor were observed (at 64.4–64.7 ppm, Fig. 2) in the 1:0.5 and 1:1 (−)-**C7B**:CAII samples. In contrast, no free biosensor was observed in either the 1:0.5 or 1:1 (+)-**C7B**:CAII samples (Fig. 2).

These hp ^{129}Xe NMR data indicate that diastereomerism alone cannot explain the observation of two “bound” peaks in the CAII-**C7B** model system. A more compelling explanation arises from the fact that X-ray crystallographic studies with CAII showed binding of functionalized benzenesulfonamide inhibitors at both the canonical Zn^{2+} buried active site and a less buried ‘b’ site near the protein surface (37). The lack of free biosensor in the 1:0.5 (+)-**C7B**:CAII sample (Fig. 2), is consistent with (+)-**C7B** binding concurrently at both sites.

The peak observed at 72 ppm for CAII:(−)-**C7B** remains particularly striking as this represents a significant chemical shift change relative to the “free” biosensor peak at 64 ppm. In this example, the chirality of the biosensor is very important, as it clearly affects CAII binding interactions with the cryptophane biosensor. Interestingly, this effect is seen most profoundly for the intermediate linker length (C7), as neither the C6 nor the C8 biosensor produced a CAII:^{129}Xe NMR resonance >68 ppm (33).

We hypothesize that the larger chemical shift change observed for (−)-**C7B** results from interaction with the CAII active-site pocket, leading to a significant perturbation of the xenon electron cloud within the cryptophane. This interaction could be enforced through Zn^{2+} coordination. Indeed, the greater linewidth of the ^{129}Xe NMR peaks for the CAII:(−)-**C7B** sample suggests that the protein may be restricting the motions of the cryptophane, preventing free rotation. Notably, the narrow ^{129}Xe NMR linewidths observed for the CAII:(+)-**C7B** sample make it more likely that the cryptophane, although “bound”, is freely rotating at some distance from CAII in solution, which our modeling suggests is more consistent with ‘b-site’ binding.. Further studies employing protein mutagenesis, protein crystallography, ^{129}Xe NMR biosensors and spectroscopy are underway, with the goal of elucidating these different binding modes. It remains a compelling question how specific, supramolecular interactions contribute to differences in ^{129}Xe NMR chemical shift.

Experimental

All commercially available chemicals were purchased from Sigma-Aldrich, Fisher or Acros Organics and used without further purification. All air- and moisture-sensitive reactions were performed under inert atmosphere in glassware flamed under vacuum, and using

anhydrous solvents dried by standard methods. Standard workup procedures involved multiple (~3) extractions with the indicated organic solvent, followed by washing of the combined organic extracts with water or brine, drying over Na_2SO_4 and removal of solvents *in vacuo*. Column chromatography was performed using silica gel (60 Å pore size, 40-75 μm particle size) from Sorbent Technologies. Thin layer chromatography (TLC) was performed using silica gel plates (60 Å pore size, Whatman) with UV light at 254 nm as the detection method. High resolution mass spectrometry (HRMS) data were obtained using electrospray ionization (ESI) mass spectrometry on a Micromass Autospec at the Mass Spectrometry Center in the University of Pennsylvania Chemistry Department. ^{1}H NMR (360 and 500 MHz) and ^{13}C NMR (90 and 125 MHz) spectra were obtained on Bruker DMX 360 and AMX 500 spectrometers in the same department. Electronic circular dichroism (ECD) spectra were recorded at 298 K on a Chirascan™ ECD spectrometer using cells with a 0.1-cm pathlength. An in-house ^{129}Xe hyperpolarizer based on the IGI.Xe.2000 system (Nycomed-Amersham, GE). Hyperpolarizer gas supply, purchased from Concorde Gases, NJ, was a mixture of 89% N_2, 10% He, and 1% natural isotopic abundance Xe (26.4% ^{129}Xe). ^{129}Xe atoms were hyperpolarized to 10-15% after cryogenic separation, accumulation, thawing, and collection in degassed airtight NMR tubes (New Era) (33). These steps yielded 2-3 atm of hyperpolarized Xe in the tube. After hp ^{129}Xe was collected, NMR tubes were shaken to mix hp ^{129}Xe gas with biosensor solutions. All ^{129}Xe NMR spectra were acquired on a 500 MHz Bruker BioDRX NMR spectrometer at the University of Pennsylvania NMR Facility. Radio-frequency pulse frequency for ^{129}Xe was 138.12 MHz. Samples were observed using a Bruker 10 mm PABBO NMR probe. ^{129}Xe spectra were processed using standard protocols from Bruker, and calibration was done by the same protocol as previous ^{129}Xe NMR spectra of carbonic anhydrase biosensor solutions (33). NMR peak intensities were adjusted for best visibility relative to background.

Synthesis of enantiopure cryptophane biosensors

Precursors **1a**, **1b** and linker 4-(azidomethyl)-benzenesulfonamide **2**, were prepared following published protocols from our laboratory (31, 33). 3-Azidopropionic acid **4** was prepared by a literature procedure and it matched the reported ^{1}H NMR spectrum (38).

Cryptophane (−)-**3a:** Compound **1a** (0.031 g, 0.032 mmol, 1 equiv.) was dissolved in dry DMSO (0.8 mL) at rt with stirring. Sulfonamide linker **2** (0.006 g, 0.03 mmol, 0.9 equiv.) dissolved in DMSO (0.2 mL) was added. $CuSO_4$ (0.003 g, 0.02 mmol, 0.5 equiv., in 12 μL water) was added, followed by 2,6-lutidine (1 equiv., d = 0.925 g/mL), and (+)-sodium-L-ascorbate (0.062 g, 0.31 mmol, 10 equiv., in 45 μL water). The reaction was allowed to stir overnight and then poured into H_2O (5 mL). This solution was extracted 3 times with ethyl acetate followed by standard workup. The yellow oil recovered was purified by silica gel column chromatography ($CH_2Cl_2 \rightarrow$THF:CH_2Cl_2 30:70, *v/v*) to give the pure product **3a (**0.017 g, 0.014 mmol, 45% yield) as a white solid. ^{1}H NMR and ^{13}C NMR spectra for **3a** were identical to the spectra of the corresponding racemic (±) compound (33). Confirmation of compound identity came from HRMS (m/z): $[M+Na]^+$ calcd. for $C_{67}H_{62}N_4O_{14}SNa$ 1201.3881; found, 1201.3862.

Cryptophane (+)-**3b:** Following the procedure for the synthesis of (−)-**3a**, compound **1b** (0.031 g, 0.032 mmol, 1 equiv.) reacted with the sulfonamide linker **2** in dry DMSO (1 mL) in the presence of $CuSO_4$ (0.003 g, 0.02 mmol, 0.5 equiv., in 12 μL water), 2,6-lutidine (1 equiv., d = 0.925 g/mL), and (+)-sodium-L-ascorbate (0.062 g, 0.31 mmol, 10 equiv., in 45 μL water) to give 0.018 g (0.015 mmol, 47% yield) of (+)-**3b** as a white solid. ^{1}H NMR and ^{13}C NMR spectra for **3b** were identical to the spectra of **3a** and the corresponding racemic (±) compound (33). Confirmation of compound identity came from HRMS (m/z): $[M+H]^+$ calcd. for $C_{67}H_{63}N_4O_{14}S$ 1179.4062; found, 1179.4133.

(−)-C7B: Following the same cycloaddition procedure, compound **3a** (0.015 g, 0.013 mmol, 1 equiv.) reacted with the linker **4** in dry DMSO (0.8 mL) in the presence of $CuSO_4$ (0.001 g, 0.009 mmol, 0.5 equiv., in 10 μL water), 2,6-lutidine (1 equiv., d = 0.925 g/mL), and (+)-sodium-L-ascorbate (0.025 g, 0.13 mmol, 10 equiv., in 35 μL water) to give 0.009 g (0.006 mmol, 49% yield) of (−)-**C7B** as a white solid. Pure product was extracted with ethyl acetate followed by standard workup without the need for column chromatography purification. ^{1}H NMR and ^{13}C NMR spectra for (−)-**C7B** are identical to the spectra of the corresponding racemic (±) compound. HRMS (m/z) confirmed compound identity: $[M-H]^+$ calcd. for $C_{73}H_{71}N_{10}O_{18}S$ 1407.4669; found, 1407.4666.

(+)-C7B: Following the same cycloaddition procedure, compound **3b** (0.015 g, 0.013 mmol, 1 equiv.) reacted with the linker **7** in dry DMSO (0.8 mL) in the presence of $CuSO_4$ (0.001 g, 0.009 mmol, 0.5 equiv., in 10 μL of water), 2,6-lutidine (1 equiv., d = 0.925 g/mL), and (+)-sodium-L-ascorbate (0.025 g, 0.13 mmol, 10 equiv., in 35 μL water) to give 0.01 g (0.007 mmol, 51% yield) of (+)-**C7B** as a white solid. Pure product was extracted with ethyl acetate followed by standard workup without the need for the column chromatography purification. ^{1}H NMR and ^{13}C NMR spectra for (+)-**C7B** were identical to the spectra of (−)-**C7B** and the corresponding racemic (±) compound (33). HRMS (m/z) confirmed compound identity: $[M-H]^+$ calcd. for $C_{73}H_{71}N_{10}O_{18}S$ 1407.4669; found, 1407.4698.

Conclusions

We described the 12-step synthesis, characterization and application of enantiopure **C7B** biosensors. The use of enantiopure biosensors helped to clarify the assignment of multiple "CAII-bound" ^{129}Xe NMR peaks. These studies show that diastereomerism alone cannot explain the multiple peaks observed for the racemic C7B:CAII sample, as ^{129}Xe NMR peaks positioned at 68 and 72 ppm were similarly observed for (−)-**C7B**:CAII sample. We hypothesize that these different peaks arise instead from interactions at two different benzenesulfonamide binding sites in CAII that were previously identified by X-ray crystallography (37). This study highlights a role for hp ^{129}Xe NMR spectroscopy to investigate supramolecular interactions involving protein-ligand binding.

Guided by numerous crystal structures of CAII-inhibitor complexes, CAII has served as a useful model system for rational drug design (32, 39, 40). These inhibitor studies have largely focused on binding benzenesulfonamide moieties to the buried Zn^{2+} active site. The current study raises interesting questions about the relative occupancy of benzenesulfonamide inhibitors at multiple CAII binding sites.

Acknowledgments

This work was supported by the National Institutes of Health under Grant [GM097478] and the UPenn Chemistry Department. We thank George Furst (Chemistry Department, University of Pennsylvania) for NMR support.

References

1. Degani H, Gusis V, Weinstein D, Fields S, Strano S. Nature Med. 1997; 3:780–782. [PubMed: 9212107]
2. Foster-Gareau P, Heyn C, Alejski A, Rutt BK. Magn. Reson. Med. 2003; 49:968–971. [PubMed: 12704781]
3. Hancu I, Dixon WT, Woods M, Vinogradov E, Sherry AD, Lenkinski RE. Acta Radiol. 2010; 51:910–923. [PubMed: 20828299]
4. Woods M, Woessner DE, Sherry AD. Chem. Soc. Rev. 2006; 35:500–511. [PubMed: 16729144]
5. Aime S, Castelli DD, Terreno E. Angew. Chem.-Int. Edit. 2005; 44:5513–5515.
6. Schroder L, Lowery TJ, Hilty C, Wemmer DE, Pines A. Science. 2006; 314:446–449. [PubMed: 17053143]
7. Bai Y, Hill AP, Dmochowski IJ. Anal. Chem. 2012; 84:9935–9941. [PubMed: 23106513]
8. Nikolaou P, Coffey AM, Walkup LL, Gust BM, Whiting N, Newton H, Barcus S, Muradyan I, Dabaghyan M, Moroz GD, Rosen MS, Patz S, Barlow MJ, Chekmenev EY, Goodson BM. Proc. Natl. Acad. Sci. U. S. A. 2013; 110:14150–14155. [PubMed: 23946420]
9. Cherubini A, Bifone A. Prog. Nucl. Magn. Reson. Spec. 2003; 42:1–30.
10. Collet A. Comp. Supramol. Chem. 1996; 2:325–365.
11. Brotin T, Dutasta JP. Eur. J. Org. Chem. 2003; 6:973–984.
12. Bartik K, Luhmer M, Dutasta JP, Collet A, Reisse J. J. Am. Chem. Soc. 1998; 120:784–791.
13. Jacobson DR, Khan NS, Collé R, Fitzgerald R, Laureano-Pérez L, Bai Y, Dmochowski IJ. Proc. Natl. Acad. Sci. U.S.A. 2011; 108:10969–10973. [PubMed: 21690357]
14. Taratula O, Hill PA, Khan N, Carroll PJ, Dmochowski IJ. Nature Commun. 2010; 1 doi:10.1038/ncomms1151.
15. Hill PA, Wei Q, Troxler T, Dmochowski IJ. J. Am. Chem. Soc. 2009; 131:3069–3077. [PubMed: 19239271]
16. Taratula O, Dmochowski IJ. Curr. Opin. Chem. Biol. 2010; 14:97–104. [PubMed: 19914122]
17. Brotin T, Dutasta J-P. Chem. Rev. 2009; 109:88–130. [PubMed: 19086781]
18. Schröder L. Phys. Medica. 2013; 29:3–16.
19. Wei Q, Seward GK, Hill PA, Patton B, Dimitrov IE, Kuzma NN, Dmochowski IJ. J. Am. Chem. Soc. 2006; 128:13274–13283. [PubMed: 17017809]
20. Hill PA, Wei Q, Eckenhoff RG, Dmochowski IJ. J. Am. Chem. Soc. 2007; 129:9262–9263. [PubMed: 17616197]
21. Spence MM, Rubin SM, Dimitrov IE, Ruiz EJ, Wemmer DE, Pines A, Yao SQ, Tian F, Schultz PG. Proc. Natl. Acad. Sci. U. S. A. 2001; 98:10654–10657. [PubMed: 11535830]
22. Spence MM, Ruiz EJ, Rubin SM, Lowery TJ, Winssinger N, Schultz PG, Wemmer DE, Pines A. J. Am. Chem. Soc. 2004; 126:15287–15294. [PubMed: 15548026]
23. Baumer D, Brunner E, Blümler P, Zänker PP, Spiess HW. Angew. Chem.-Int. Edit. 2006; 45:7282–7284.
24. Driehuys B, Moller HE, Cleveland ZI, Pollaro J, Hedlund LW. Radiology. 2009; 252:386–393. [PubMed: 19703880]
25. Boutin C, Desvaux H, Carrière M, Leteurtre F, Jamin N, Boulard Y, Berthault P. NMR Biomed. 2011; 24:1264–1269. [PubMed: 22223364]
26. Boutin C, Stopin A, Lenda F, Brotin T, Dutasta J-P, Jamin N, Sanson A, Boulard Y, Leteurtre F, Huber G, Bogaert-Buchmann A, Tassali N, Desvaux H, Carrière M, Berthault P. Bioorg. Med. Chem. 2011; 19:4135–4143. [PubMed: 21605977]

27. Zhou X, Graziani D, Pines A. Proc. Natl. Acad. Sci. U. S. A. 2009; 106:16903–16906. [PubMed: 19805177]
28. Meldrum T, Seim KL, Bajaj VS, Palaniappan KK, Wu W, Francis MB, Wemmer DE, Pines A. J. Am. Chem. Soc. 2010; 132:5936–5937. [PubMed: 20392049]
29. Mugler JP, Altes TA, Ruset IC, Dregely IM, Mata JF, Miller GW, Ketel S, Ketel J, Hersman FW, Ruppert K. Proc. Natl. Acad. Sci. U. S. A. 2010; 107:21707–21712. [PubMed: 21098267]
30. Taratula O, Hill PA, Bai Y, Khan NS, Dmochowski IJ. Org. Lett. 2011; 13:1414–1417. [PubMed: 21332141]
31. Taratula O, Kim MP, Bai Y, Philbin JP, Dmochowski IJ. Org. Lett. 2012; 14:3580–3583. [PubMed: 22783828]
32. Supuran CT. Nature Rev. Drug. Disc. 2008; 7:168–181.
33. Chambers JM, Hill PA, Aaron JA, Han ZH, Christianson DW, Kuzma NN, Dmochowski IJ. J. Am. Chem. Soc. 2009; 131:563–569. [PubMed: 19140795]
34. Aaron JA, Chambers JM, Jude KM, Di Costanzo L, Dmochowski IJ, Christianson DW. J. Am. Chem. Soc. 2008; 130:6942–6943. [PubMed: 18461940]
35. Cavagnat D, Buffeteau T, Brotin T. J. Org. Chem. 2008; 73:66–75. [PubMed: 18052292]
36. Canceill J, Collet A, Gottarelli G, Palmieri P. J. Am. Chem. Soc. 1987; 109:6454–6464.
37. Jude KM, Banerjee AL, Haldar MK, Manokaran S, Roy B, Mallik S, Srivastava DK, Christianson DW. J. Am. Chem. Soc. 2006; 128:3011–3018. [PubMed: 16506782]
38. Zhang L, Chen X, Peng X, Herman HYS, Williams ID, Sharpless KB, Fokin VV, Gouchen J. J. Am. Chem. Soc. 2005; 127:15998–15999. [PubMed: 16287266]
39. Greer J, Erickson JW, Baldwin JJ, Varney MD. J. Med. Chem. 1994; 37:1035 – 1054. [PubMed: 8164249]
40. Krishnamurthy VM, Kaufman GK, Urbach AR, Gitlin I, Gudiksen KL, Weibel DB, Whitesides GM. Chem. Rev. 2008; 108:946–1051. [PubMed: 18335973]

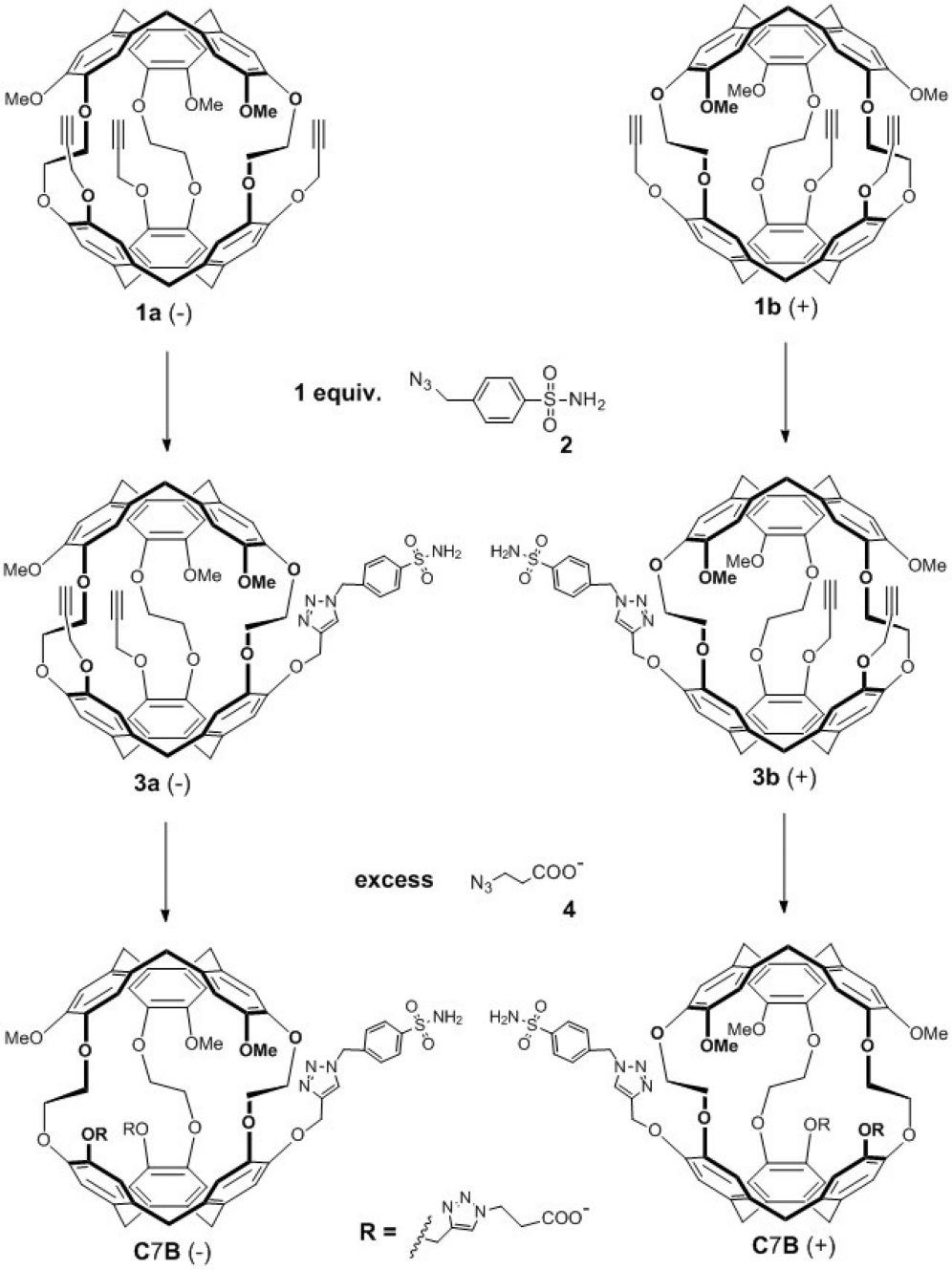

Scheme 1.

Synthesis of enantiopure cryptophane biosensors (−) and (+) **C7B** from enantiopure tripropargyl cryptophanes (**1a**, **1b**).

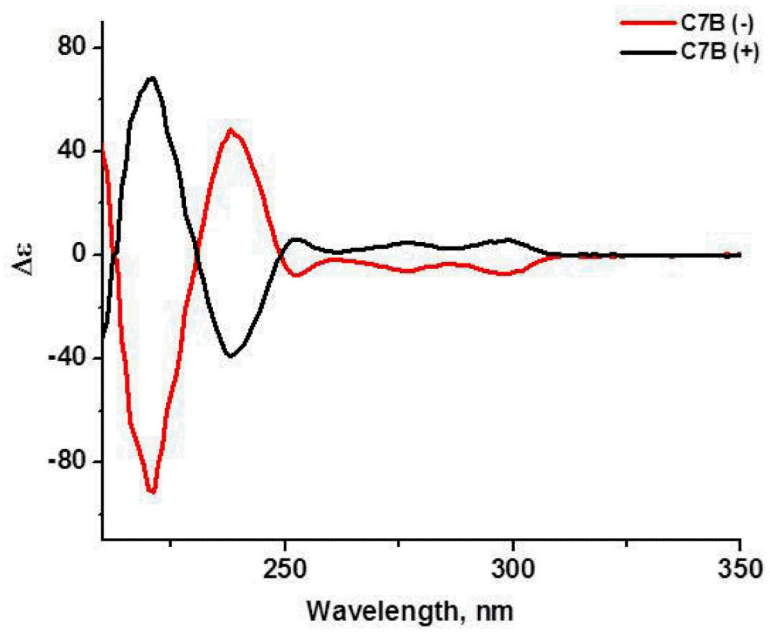

Figure 1.

ECD spectra of enantiopure biosensors (−)-**C7B** and (+)-**C7B** in 1,4-dioxane at 298 K. Molar ellipticity (Δε) has units of $M^{-1}Lcm^{-1}$.

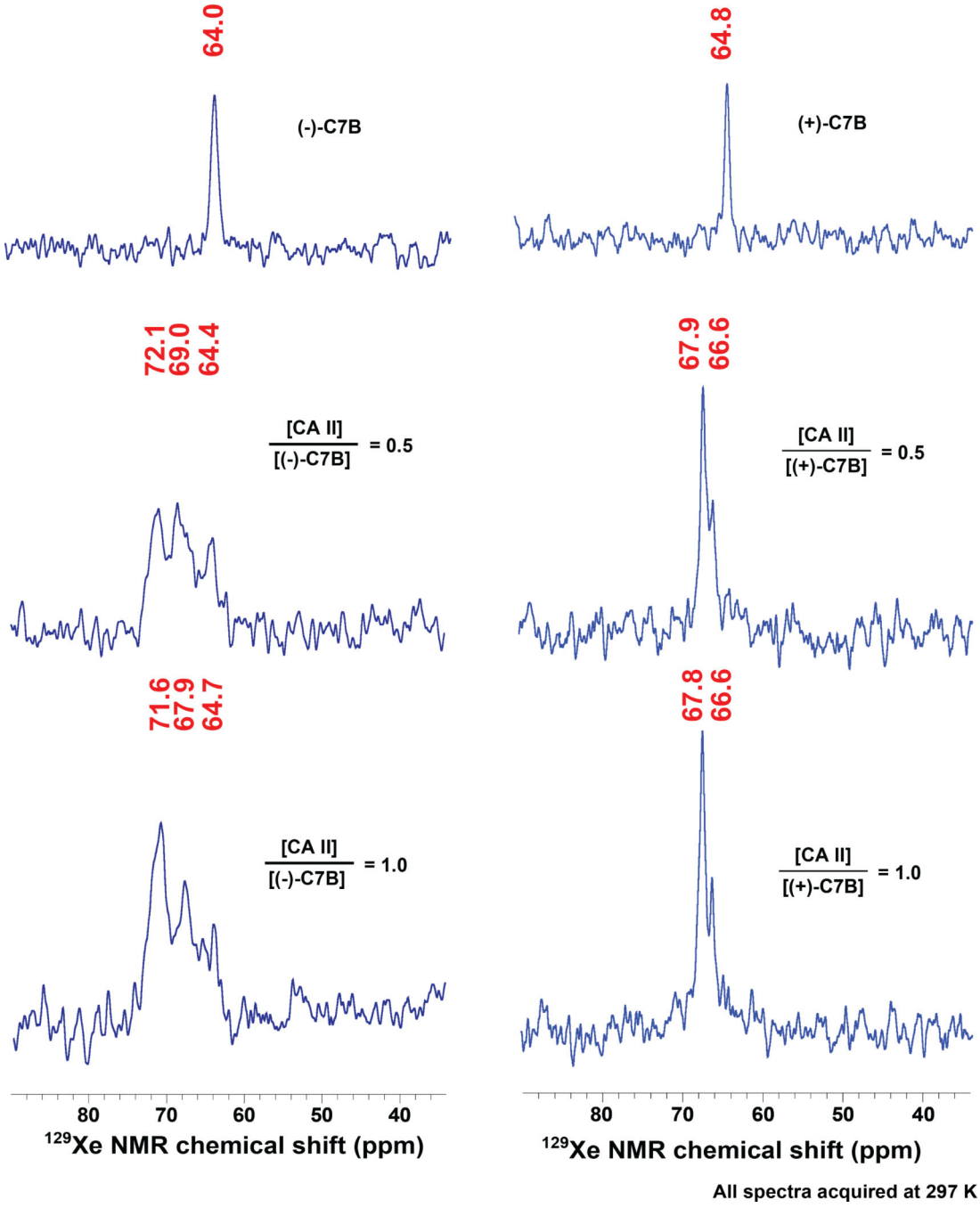

Figure 2.

HP ^{129}Xe NMR spectra of (−)-**C7B** (left column) or (+)-**C7B** (right column) before and after binding to wild-type carbonic anhydrase II. The first row shows spectra of biosensors (138 μM, (−)-**C7B**; 147 μM (+)-**C7B**) dissolved in 90% Tris-SO_4 buffer (50 mM, pH 8.0) and 10% glycerol. The second and third rows show spectra for biosensor-CA II binding. Solutions of 1.3 mM CA II in 50 mM Tris-SO_4 buffer were titrated with 0.5 and 1.0 equivalents of biosensor, respectively.

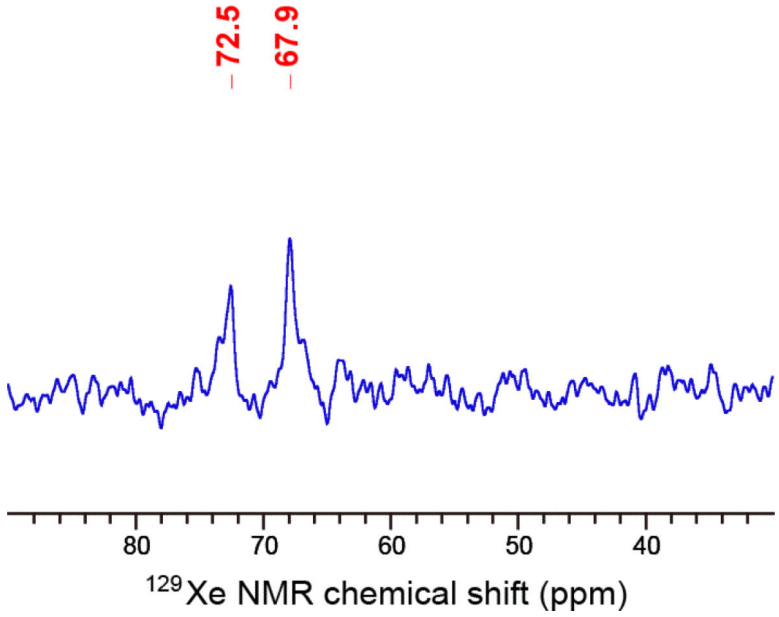

Figure 3.

HP ^{129}Xe NMR spectra of racemic **C7B** binding to wild-type carbonic anhydrase II. The **C7B** biosensor (176 μM) was dissolved in Tris-SO_4 buffer (50 mM, pH 8.0) and 10% glycerol. Solution of 1.3 mM CAII in matched Tris-SO_4 buffer was titrated to give 1:1 stoichiometry with racemic **C7B**. The chemical shifts for the two “bound” peaks (72.5, 67.9 ppm) are somewhat shifted from the spectrum in reference [33] due to differences in buffer conditions.